

# FRACTAL PARAMETERS OF PORE SPACE FROM CT IMAGES OF SOILS UNDER CONTRASTING MANAGEMENT PRACTICES

F. J. MUÑOZ, F. SAN JOSÉ MARTÍNEZ  
and F. J. CANIEGO

## Abstract

Soil structure plays an important role in flow and transport phenomena, and a quantitative characterization of the spatial heterogeneity of the pore space geometry is beneficial for prediction of soil physical properties. Morphological features such as pore-size distribution, pore space volume or pore–solid surface can be altered by different soil management practices. Irregularity of these features and their changes can be described using fractal geometry. In this study, we focus primarily on the characterization of soil pore space as a 3D geometrical shape by fractal analysis and on the ability of fractal dimensions to differentiate between two *a priori* different soil structures. We analyze X-ray computed tomography (CT) images of soils samples from two nearby areas with contrasting management practices. Within these two different soil systems, samples were collected from three depths. Fractal dimensions of the pore-size distributions were different depending on soil use and averaged values also differed at each depth. Fractal dimensions of the volume and surface of the pore space were lower in the tilled soil than in the natural soil but their standard deviations were higher in the former as compared to the latter. Also,

it was observed that soil use was a factor that had a statistically significant effect on fractal parameters. Fractal parameters provide useful complementary information about changes in soil structure due to changes in soil management.

*Keywords:* Soil Tomography; Fractal Analysis; Soil Pore Space; Soil Management Practices.

## 1. INTRODUCTION

The spatial arrangement of soil constituents — usually referred to as soil structure — controls important physical and biological processes in soil–plant–microbial systems such as moisture retention, root development or transport of water and nutrients.<sup>1</sup> For many decades, soil scientists have tried to relate structural parameters of pore geometry with physical features. Vogel and Roth<sup>2</sup> identify structural properties that are essential for inferring hydraulic properties. Vogel<sup>3</sup> studied the influence of topological characteristics of porous media and showed the significance of pore space topology for hydraulic properties. Bastardie *et al.*<sup>4</sup> used X-ray computed tomography (CT) to characterize pores accessed by earthworms. Luo *et al.*<sup>5</sup> quantified the relationship between soil macropore features such as tortuosity or network density with flow and transport phenomena.

One of the major effects of tillage and farming practices is the alteration of soil structure and, hence, the processes involved.<sup>6,7</sup> There is an interest in describing good soil management practices and deriving indicators of soil health to help in this task.<sup>8</sup> Moreover, it is imperative to improve quantitative techniques so that policy makers and practitioners can develop and implement good policies and practices.

It has been shown that X-ray CT is a very useful technique for quantifying and characterizing soil structure. This is because this technique allows the rendering and the computational processing of the 3D geometry of the pore structure. Thus, this technology provides geometrical measurements on 3D digital images of the soil pore space. Perret *et al.*<sup>9</sup> carried out a quantification of macropore networks providing numerical density, length, inclination and tortuosity of pores. Gantzer and Anderson<sup>10</sup> showed differences of the pore structure in tomographic images of soil samples under two different agricultural treatments. Luo *et al.*<sup>5</sup> obtained macropore attributes such as macroporosity, length density, network density and hydraulic radius using X-ray CT. San Jose Martinez *et al.*<sup>11</sup> analyzed CT images

of soil columns to characterize different soil structures with Minkowski functionals. Other works like Gibson *et al.*,<sup>12</sup> went deeper into the fractal analysis and showed the usefulness of this approach.

In this work, we propose a set of fractal parameters to characterize soil structure through the fractal analysis of soil pore space as a 3D geometrical shape. Our study aims to quantify the complexity of pore space geometry on CT images of intact soil columns from contrasting management practices by the following fractal parameters: fractal dimensions of the volume and the boundary surface of the pore space, which characterize how the volume and the surface of pores fills the space, and the fractal dimension of the pore size distribution, which characterizes the relationship between pore size classes.

## 2. THEORY

Fractal geometry, introduced by Mandelbrot,<sup>13</sup> can be used to describe many irregular and fragmented patterns of nature. In soil, fractals dimensions of pore space, pore–solid interface and pore size distribution are indicators of soil structure complexity.<sup>14,15</sup>

The box counting algorithm is commonly used to estimate fractal dimensions. This algorithm operates as follows. To estimate volume fractal dimension (VFD) and surface fractal dimension (SFD), the object (or its surface) is covered with a 3D lattice consisting of cubes of side  $\varepsilon$  and then the number of boxes,  $N(\varepsilon)$ , that intersect the object (or its surface) is counted. The number of boxes will vary with the size of the box  $\varepsilon$  according to the relationship

$$N(\varepsilon) \propto \varepsilon^{-D_b},$$

where  $\propto$  stands for asymptotic behavior as  $\varepsilon$  approaches zero and  $D_b$  is the estimated fractal dimension of the object (or its surface). Figures 1a and 1b show how the box counting algorithm operates to estimate VFD and SFD, respectively, on a 2D image of a soil sample. VFD and

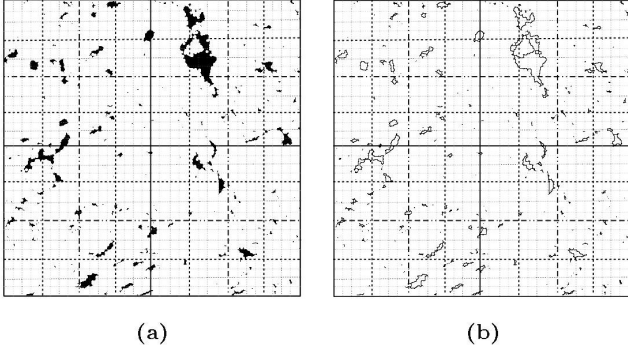


**Fig. 1** Example of the box counting algorithm in a 2D setting of (a) the area of the pores of a soil sample and (b) the boundary of the pores of the same soil sample.

SFD values would be expected to range between 2 and 3 for 3D shapes, and the VFD of a particular object should be higher than its SFD. Fractal dimension VFD measures the space-filling properties of the pore volume as a mass distribution, while the fractal dimension SFD is an indicator of the roughness of its boundary surface.

The distribution of the number of elements or different parts of an object that exhibits a fractal behavior can also be analyzed by its scaling behavior. For this analysis the numerical relationship between sizes of different parts forming the fractal object is taken into account. It has been shown<sup>16</sup> that the number-size distribution of pores displays a fractal behavior which leads to the power law scaling:

$$N_p(r > x) = kx^{-\alpha},$$

Where  $N_p(r > x)$  is the cumulative number of pores larger than  $r$ ,  $k$  is a proportionality constant and  $\alpha > 0$  is the fractal dimension of the pore size distribution<sup>14</sup> that we will call number fractal dimension (NFD) to stress the fact that it corresponds to the number-size distribution. This parameter indicates the rate of decrease in the number of pores for increasing radius. Higher  $\alpha$ 's would be consistent with a relatively lower number of larger pores.

### 3. MATERIALS AND METHODS

#### 3.1. Soil Study and Sampling

Soil samples were collected in December 2008 in two areas within an experimental farm belonging to “Instituto Madrileño de Investigación y Desarrollo Rural, Agrario y Alimentario” located in Madrid, Spain. The first sampled area (labeled T), with coordinates (WGS84) 40° 31'29" N, 3°

17'30" W, was an agricultural area under a cotton crop (*Gossypium* sp.). The soil in this area was identified<sup>17</sup> as Calcic Haploxeralf according to the USDA classification,<sup>18</sup> the textural class of the soil is clay loam, with the following proportions of constituents: 3.4% sand, 35.8% silt, 60.8% clay and 1.62% Organic Matter. The depth of the tillage was about 25 cm. The second sampled area (labeled N), with coordinates (WGS84) 40° 31'6" N, 3° 17'21" W, is a natural site (riparian vegetation: *Tamarix* sp., *Ulmus* sp.), located on a terrace of the Henares river. The soil in this second area was been identified<sup>17</sup> as Typic Xerofluvent according to the USDA classification.<sup>18</sup> The textural class of this soil was silty clay loam with the following proportions of constituents: 12.3% sand, 60.8% silt, 26.9% clay and 0.85% organic matter.

In order to extract and preserve the undisturbed samples, methacrylate cylindrical containers were used. The dimensions of the containers were 3 cm height, 2.6 cm inner diameter and 2 mm thickness. Soil samples were taken at three depths, with a difference between depths of about 10 cm; the bottom of the first group of containers was about 4 cm from the surface. In total, 24 samples were extracted, 12 in each soil area with a total of 4 replicates in each depth.

#### 3.2. Image Acquisition, Image Processing and Estimation of Fractal Dimensions

Soil samples were scanned using an X-ray CT scanner at the laboratory of Medical Imaging and Experimental Medicine in Madrid (Spain) of the Hospital General Gregorio Marañón. The tomograph device was operated at 50 keV. The output data obtained after the reconstruction were a set of 3D unsigned 16-bit RAW images. The image was a stack of 1392 slices; each slice was an image of 1600<sup>2</sup> pixels. The pixel sizes and the spacing between sections of the images was 0.03 mm. Due to an error in the acquisition of data only 22 of the 24 samples have a final reconstructed image. The labeling of the images obtained according to the sampling area is of the form Ln1.n2 where L is the treatment — T (Tillage) or N (Natural) —, n1 is the depth — 1 is shallow, 2 is intermediate and 3 is deep — and n2 is the repetition.

The image processing was performed with the public domain program ImageJ version 1.47v developed at the National Institute of Health.<sup>19</sup> The

format of the images was changed from RAW to TIFF. Firstly, images were thresholded in order to classify the entire image into two regions, the void phase of the sample (object or foreground), and the solid phase of the sample (background). The thresholding method was based on the mean operation. This local thresholding method was chosen for its stability and high performance.<sup>20</sup> The method works as follows: for each pixel  $x$  of the image a threshold is calculated, if the pixel value is below the threshold then  $x$  is classified as background, otherwise it is classified as object. The selection of the threshold for each pixel  $x$  is made by examining the pixel values of the surroundings of  $x$ . For this work, the surrounding pixels were those at a distance of 3 mm (100 pixels) or less from the selected pixel  $x$ .

Images were filtered in order to reduce Gaussian noise and artifacts. These effects arise during the tomographic scan due to defects in the X-ray beam and in the detector.<sup>21</sup> The chosen filter was a spatial filter that uses the maximum function with radius  $r$ . The filtering operates on each image pixel as follows: each pixel  $x$  in the original image is replaced by the maximum of the values of the pixels covered by the disk of radius  $r$  (two pixels in our case) centered on the pixel  $x$ .

A cubic region of  $512^3$  voxels was selected from each 3D picture. This region corresponds to a cube whose edge has an actual length of 15.36 mm. This size was chosen to avoid voxels belonging to the container or voxels representing soil near the sampling tube that might have been damaged during sampling. Figures 2a and 2b show the 3D reconstructions of the pore space of a sample of the natural area soil and the pore space of a sample of the agrosystem soil, respectively.

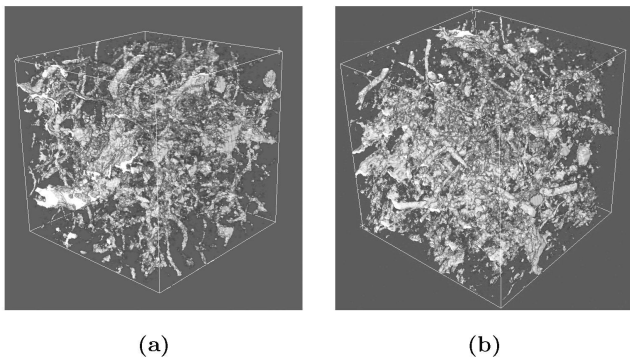


**Fig. 2** Two examples of 3D rendering of the pore space of a soil core from (a) a natural soil (N2\_2) and (b) a tilled soil (T2\_2).

The VFD and SFD were estimated using the box counting algorithm. For this, Fractal Count Plugin<sup>22</sup> was used. The box counting technique has been applied to estimate the VFD by counting the boxes that intersect the voxels representing the pores in each cube. An estimate of the SFD was obtained by counting only the boxes that intersect the voxels of the boundary of the pore space. The boundary surface was obtained with the outline operation as shown in Fig. 1b for a 2D image. The number of sizes of boxes used in the algorithm was 9, which followed a geometric sequence corresponding to edges lengths of 512, 256,  $\dots$ , 2, and 1 voxels.

The pore-size distribution was generated by morphological granulometry. We describe the technique below for 2D images to illustrate the ideas behind it. Figures 3a–3d show an example of how this method operates on a 2D image of a soil. Overall, this technique removes pores smaller than a certain size  $r$  and, then, it evaluates the volume (or area in 2D case) of the remaining pores. The pore size criterion used in this work corresponds with the hydraulic radius concept.<sup>23</sup> Morphological granulometry is based on two basic morphological operations<sup>24</sup>: erosion and dilation. First, the erosion of radius  $r$  produces a reduction of size  $r$  of the pores; secondly, the dilation of radius  $r$  produces the corresponding growth. The application

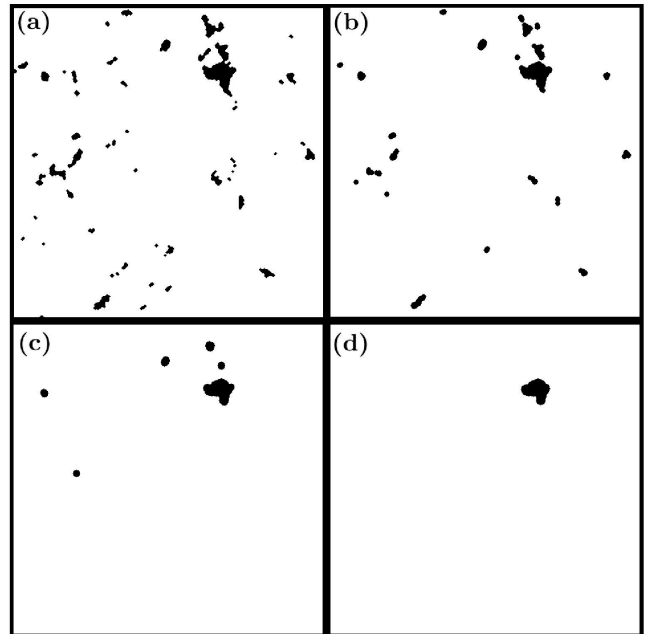


**Fig. 3** Example of the morphological granulometry technique in a 2D setting. At different stages of the process (a), (b), (c), (d) pores smaller than a certain radius  $r$  are removed to measure the area of the remaining pores.

of these two consecutive operations removes pores smaller than  $r$ . They disappear during the erosion and they are not recovered during the dilation but pores with sizes larger than  $r$  will not disappear with the erosion and they will recuperate their size with the dilation. The difference between the initial stage and the final stage results in the total volume of pores with size lesser than  $r$ . The successive application of this procedure, with increasing radius  $r$  provides the curve that defines the pore size distribution — i.e. the curve of the number of pores with size greater than  $r$  as a function of  $r$ .<sup>25</sup> Once the curve of the pore size distribution was obtained, the NFD was estimated as the slope of the linear fit in the log-log plot.

#### 4. RESULTS AND DISCUSSION

Figure 4 shows the log-log plot of the distributions of the number of pores  $N_p(r > x)$  with spherical equivalent radius  $r$  greater than  $x$  and the corresponding regression line of the linear fit for each sample. The correlation coefficients  $R^2$  of the fit

are greater than 0.92. On average, these values are  $0.9624 \pm 0.019$  for T and  $0.9687 \pm 0.021$  for N. As a consequence, the NFD fractal dimension is well defined and the pore size distributions of these samples display a clear fractal behavior. The values of NFD parameter (Fig. 5) range between 3.24 and 4.88 for T samples and between 3.84 and 4.56 for N samples. These high values of NFD would be seen as unrealistic, but it is worth noting that, to our knowledge, there is no 3D model of soil structure that takes account, in a unified framework, of the simultaneous fractal behavior of its solid part, its voids and their interface, and that could guide our intuition in this matter. In that respect, the 2D pore-solid fractal model of Perrier and Bird<sup>26</sup> represents an enormous progress.

The average value of NFD for T samples is slightly higher but the difference was not statistically significant. This is congruent with a lower relative number of larger pores in samples from the agrosystem as compared with samples from the natural soil. Kravchenko *et al.*<sup>27</sup> also found that samples from conventional tillage had

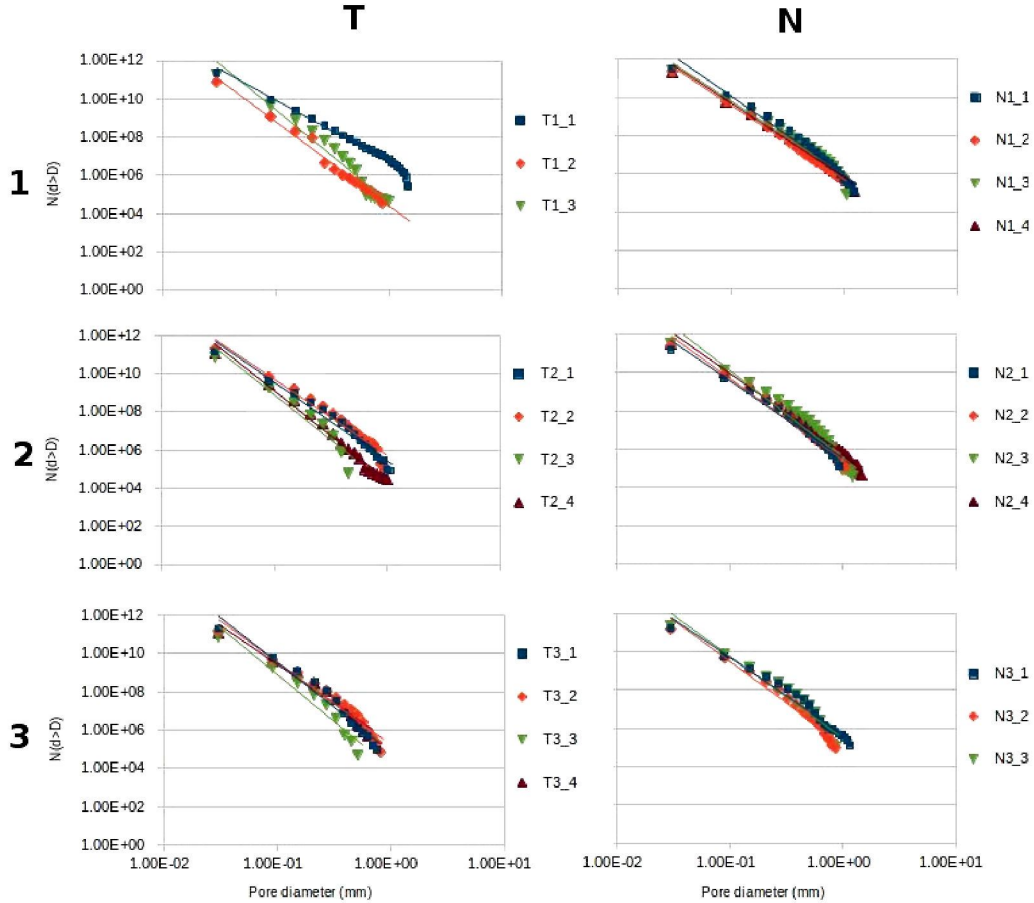
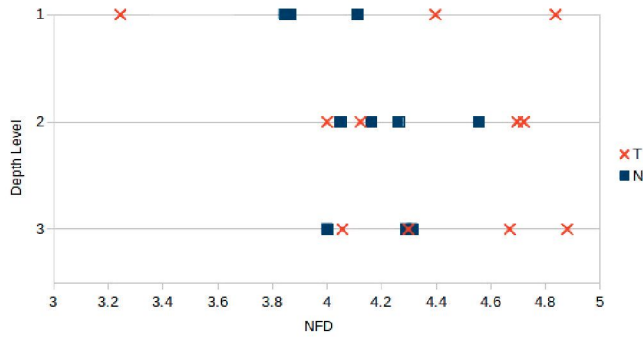


Fig. 4 Log-log plot of the curves of pore size distributions. Regression lines to evaluate NFD parameters are also shown.





**Fig. 5** Estimated values of NFD for each depth and soil treatment. Value 1 in the vertical axes of the graph corresponds to the uppermost layer of soil and number 3 to the deepest one.

a tendency for higher fractal dimensions than samples from natural soils. The mean value of NFD is also lower for N samples than for T samples in each depth, and the standard deviation is also greater for T samples than for N samples at each depth. Therefore, on average, T samples have a lower abundance of large pores at each depth and a greater variability between samples. For T samples, an increase of the NFD with depth is observed. It suggests that, the number of macropores decreases with depth in the agrosystem.

Figures 6 and 7 show estimated values of VFD and SFD. The minimum coefficient of determination  $R^2$  for VFD is 0.9762 and it is 0.9687 for SFD — they both correspond to sample T1\_2. All values of VFD and SFD are greater than 2 and lesser than 3. It can be seen that VFD values are always greater than SFD ones, having a difference of about 0.1 between them, with larger differences in N samples. The low values of VFD as compared with the dimension of the embedding space and of

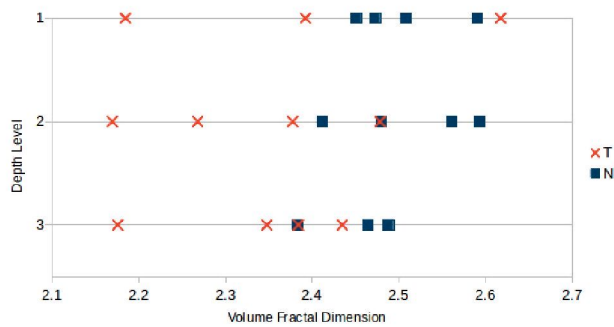


**Fig. 6** Estimated values of VFD for each depth and soil treatment. Value 1 in the vertical axes of the graph corresponds to the uppermost layer of soil and number 3 to the deepest one.

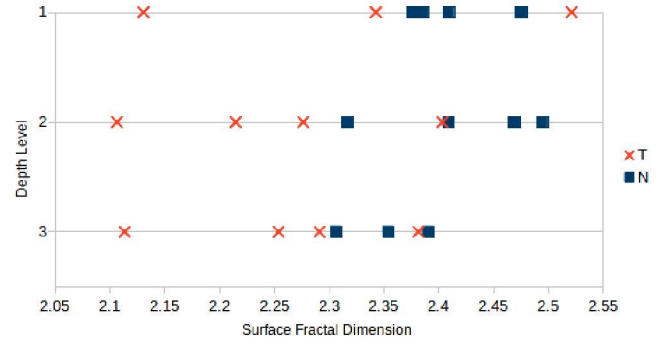


**Fig. 7** Estimated values of SFD for each depth and soil treatment. Value 1 in the vertical axes of the graph corresponds to the uppermost layer of soil and number 3 to the deepest one.

the high values of SFD as compared with the dimension of its embedding space suggest highly complex pore space geometry and extremely rough pore-soil interface. Averaged values of VFD and SFD are lower for T samples as compared with N samples for each depth. This is consistent with the results of other studies that compared the box-counting dimension of the pore space of tilled and undisturbed soils.<sup>10,27,28</sup> Let us note here that N soil samples have lower NFD and higher VFD than T samples. It might suggest that N samples display a more heterogeneous spatial distribution of voids in soil as a consequence of the presence of a larger number of macropores as compared with T samples. Moreover, the boundary surface of the pore space of the N samples also seems to have greater complexity because of its roughness. In contrast with the fractal parameter NFD, parameters VFD and SFD do not show any trend with depth. Probably, this is due to the fact that samples correspond to a narrow layer of the uppermost part of the soil. Similar results were reported by Perret *et al.*<sup>9</sup> San Jose Martinez *et al.*<sup>29</sup> used multifractal analysis of the variation of cross-sectional porosity with depth of CT images of large soil columns to characterize the porosity spatial memory. They found that the Hurst exponent of this series is congruent with persistence or positive autocorrelation. Thus, the persistence of sectional porosity could explain the absence of any trend of fractal parameters VFD and SFD with depth. The different behavior that parameters NFD show suggests the lack of a direct relationship between pore space structure and pore size distribution — different pore size distributions seem to yield pore space geometries that appear indistinguishable in this type of soils.

**Table 1** Multivariate Analysis ANOVA: Mean Squares and  $p$ -Values, for Fractal Parameters — NFD, VFD and SFD — Depending on Soil Use and Depth.

	Porosity	P-val (Porosity)	NFD	P-val (NFD)
Soil Use	23,8360	0,0705	0,2372	0,2043
Depth Level	5,8622	0,4206	0,2050	0,2497
	VFD	P-val (VFD)	SFD	P-val (SFD)
Soil Use	0,1042	0,0103	0,0824	0,0096
Depth Level	0,0057	0,6466	0,0049	0,6170

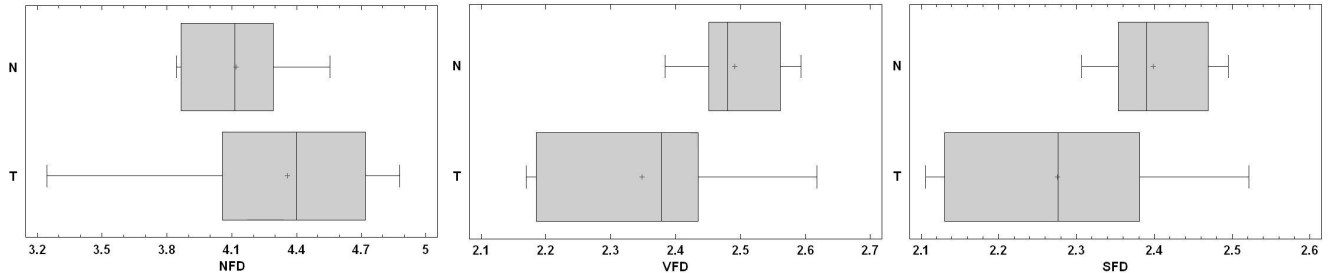


**Fig. 8** Summary of NFD, VFD and SFD values grouped by soil treatment.

Table 1 displays mean squares and  $p$ -values of the ANOVA analysis of fractals parameters — NFD, VFD and SFD — along with porosity, depending on soil use and depth. These results indicate that soil use has a statistically significant effect on VFD and SFD parameters. But depth does not seem to have any statistically significant effect on any of these parameters. Figure 8 shows a summary of the fractal parameters — VFD, SFD and NFD — for each soil use. The results of Kravchenko *et al.*<sup>27</sup> are consistent with our findings when they characterized heterogeneity in pore distribution patterns of soil aggregate — a key element of soil structure — from the same soil subject to long-term contrasting management practices. They concluded that mechanisms of aggregates formation might differ in their importance under different land use and management practices. Again, our results seem to indicate the lack of statistical significance of the effect of soils use and depth on porosity and pore size distributions as characterized by NFD. It suggests that other parameters than NFD should be investigated in order to provide a comprehensive fractal characterization of the soil pore structure.

It has been pointed out that there is a need for a detailed geometrical characterization of soil pore structure in order to better understand its role in soil functioning, including its contribution to accumulation and protection of soil organic matter, to optimization of soil water and air

regimes, and to storage and availability of plant nutrients.<sup>30</sup> Mathematical morphology<sup>23</sup> provides a set of nonfractal parameters — in the realm of classical nonfractal geometry — that has been used to characterize soil structures that were *a priori* different.<sup>11</sup> Following the rationale of this theory, a set of fractals parameters beyond VFD and SFD is needed to build an exhaustive fractal description of soil structure. The same rationale suggests the utility of measures of soil pore connectivity. Recent studies of intra-aggregate porosity with 2D images of soil sections seem to suggest that lacunarity could be a suitable fractal parameter choice.<sup>27,31,32</sup> Therefore, our findings could improve knowledge of the fractal geometry of soil pore structure with a comprehensive geometrical description with fractal attributes of soil pore space as a 3D shape. These fractals attributes should probably include, but not restricted to, VFD, SFD and lacunarity.

## 5. CONCLUSIONS

Fractal analysis provides different fractal parameters to assess and quantify the complex geometrical structure of a fractal object but fractal structures that are dissimilar to the naked eye may have the same specific fractal dimension. In this work, we focus on the ability of a set of three fractal geometrical descriptors to characterize soil structure by

parametrizing the fractal features of soil pore space geometry as a 3D shape rendered from CT images of undisturbed soil cores.

Taking into account the 3D nature of the geometrical object of interest, we explore the suitability of the fractal dimensions of the volume and the boundary surface of the pore space and of the fractal dimension of the pore size distribution as fractal indicators of soil complexity. In order to assess the value of this set of fractal parameters for soil structure discrimination, two groups of soil samples from two areas under different management soil practices — conventional tillage and natural vegetation — were compared. Within these two different soil systems, samples were collected from three depths. Fractal dimensions of the pore-size distributions were different depending on soil use and averaged values from each depth also differed. Fractal dimensions of volume and surface of the pore space were lower in the tilled soil than in the natural soil but their standard deviations were higher on the former as compared to the latter area of study. Also, it was observed that soil use was a factor that had a statistically significant effect on fractal parameters.

This study's results could improve the knowledge of the fractal geometry of soil pore structure with a comprehensive geometrical description with fractal attributes of soil pore space as a 3D shape. These fractals attributes should probably include VFD, SFD and lacunarity. Further research is needed in order to establish such a comprehensive set of fractal geometrical indicators to better understand and predict the complexity of soil functioning.

## ACKNOWLEDGMENTS

This research work was partially funded by Spain's Plan Nacional de Investigación Científica, Desarrollo e Innovación Tecnológica (I+D+I) under Ref. AGL2011-25175.

## REFERENCES

1. D. Hillel, *Environmental Soil Physics: Fundamentals, Applications, and Environmental Considerations* (Academic Press, 1998).
2. H. J. Vogel and K. Roth, A new approach for determining effective soil hydraulic functions, *Eur. J. Soil Sci.* **49**(4) (1998) 547–556.
3. H. J. Vogel, Topological characterization of porous media, in *Morphology of Condensed Matter* (Springer, Berlin, Heidelberg, 2002), pp. 75–92.
4. F. Bastardie, Y. Capowiez, J. R. De Dreuzay and D. Cluzeau, X-ray tomographic and hydraulic characterization of burrowing by three earthworm species in repacked soil cores, *Appl. Soil Ecol.* **24**(1) (2003) 3–16.
5. L. Luo, H. Lin and J. Schmidt, Quantitative relationships between soil macropore characteristics and preferential flow and transport, *Soil Sci. Soc. Am. J.* **74**(6) (2010) 1929–1937.
6. C. J. Bronick and R. Lal, Soil structure and management: A review, *Geoderma* **124**(1) (2005) 3–22.
7. L. Brussaard, P. C. De Ruiter and G. G. Brown, Soil biodiversity for agricultural sustainability, *Agric. Ecosyst. Environ.* **121**(3) (2007) 233–244.
8. J. W. Doran and M. R. Zeiss, Soil health and sustainability: Managing the biotic component of soil quality, *Appl. Soil Ecol.* **15**(1) (2000) 3–11.
9. J. S. Perret, S. O. Prasher and A. R. Kacimov, Mass fractal dimension of soil macropores using computed tomography: From the box-counting to the cube-counting algorithm, *Eur. J. Soil Sci.* **54** (2003) 569–579.
10. C. J. Gantzer and S. H. Anderson, Computed tomographic measurement of macroporosity in chisel-disk and no-tillage seedbeds, *Soil Tillage Res.* **64** (2002) 101–111.
11. F. San José Martínez, F. J. Muñoz, F. J. Caniego and F. Peregrina, Morphological functions to quantify three-dimensional tomograms of macropore structure in a vineyard soil with two different management regimes, *Vadose Zone J.* **12**(3) (2013), DOI: 10.2136/vzj2012.0208.
12. J. R. Gibson, H. Lin and M. A. Bruns, A comparison of fractal analytical methods on 2- and 3-dimensional computed tomographic scans of soil aggregates, *Geoderma* **134**(3) (2006) 335–348.
13. B. B. Mandelbrot, *Les Objets Fractals: Forme, Hasard et Dimension* (Flammarion, Paris, France, 1975).
14. A. N. Anderson, A. B. McBratney and J. W. Crawford, Applications of fractals to soil studies, *Adv. Agron.* **63** (1998) 1–76.
15. E. Perfect and B. D. Kay, Application of fractals in soil and tillage research, *Soil Tillage Res.* **36** (1995) 1–20.
16. S. Diamond, Pore size distributions in clays, *Clays Clay Miner.* **18** (1970) 7–23.
17. INIA, El Encín, suelo y clima. INIA-MAPA (1977), Madrid, p. 213.
18. Soil Survey Staff, *Keys to Soil Taxonomy*, 11th edn. (USDA-Natural Resources Conservation Service, Washington, DC, 2010).
19. W. S. Rasband, Image J. US National Institutes of Health, Bethesda, MD, USA (1997).
20. P. Iassonov, T. Gebrenegus and M. Tuller, Segmentation of X-ray computed tomography images of



- porous materials: A crucial step for characterization and quantitative analysis of pore structures, *Water Resour. Res.* **45**(9), doi:10.1029/2009WR008087 (2009).
21. R. A. Ketcham and W. D. Carlson, Acquisition, optimization and interpretation of X-ray computed tomographic imagery: Applications to the geosciences, *Comput. Geosci.* **27**(4) (2001) 381–400.
  22. J. Bache-Wiig and P. C. Henden, Measurements on microtomographic images of fibrous structures, Doctoral Dissertation, Masters Thesis, Norwegian University of Science and Technology (2004), Available at <http://www.pvv.org/~perchrh/papers>.
  23. H. J. Vogel and K. Roth, Quantitative morphology and network representation of soil pore structure, *Adv. Water Res.* **24**(3) (2001) 233–242.
  24. J. Serra, *Image Analysis and Mathematical Morphology*, Vol. 1 (Academic Press, 1982).
  25. J. Ohser and F. Mücklich, *Statistical Analysis of Microstructures in Materials Science* (Wiley, Chichester, 2000).
  26. E. M. A. Perrier and N. R. A. Bird, Modeling soil fragmentation: The pore solid fractal approach, *Soil Tillage Res.* **64** (2002) 91–99.
  27. A. N. Kravchenko, W. Wang, A. J. M. Smucker and M. L. Rivers, Long-term differences in tillage and land use affect intra-aggregate pore heterogeneity, *Soil Sci. Soc. Am. J.* **75** (2011) 1658–1666.
  28. H. C. Chun, D. Giménez and S. W. Yoon, Morphology, lacunarity and entropy of intra-aggregate pores: Aggregate size and soil management effects, *Geoderma* **146** (2008) 83–93.
  29. F. San José Martínez, M. A. Martín, F. J. Caniego, M. Tuller, A. Guber, Y. Pachepsky and C. García-Gutiérrez, Multifractal analysis of discretized X-ray CT images for the characterization of soil macropore structures, *Geoderma* **156** (2010) 32–42.
  30. M. Lützow, I. V. Kögel-Knabner, K. Ekschmitt, E. Matzner, G. Guggenberger, B. Marschner and H. Flessa, Stabilization of organic matter in temperate soils: Mechanisms and their relevance under different soil conditions — a review, *Eur. J. Soil Sci.* **57** (2006) 426–445.
  31. M. C. Sukop, Porosity, percolation thresholds, and water retention behavior of random fractal porous media, Dissertation, University of Kentucky, Lexington, KY, p. 128 (2001).
  32. M. C. Sukop, G.-J. van Dijk, E. Perfect and W. K. P. van Loon, Percolation thresholds in 2-dimensional prefractal models of porous media, *Transp. Porous Media* **48** (2002) 187–208, Available at <http://dx.doi.org/10.1023/A:1015680828317>.